1974-02

Turbulence effects on an ambient pressure discharge

Biblarz, Oscar; Nelson, Robert E.

Journal of Applied Physics, Vol. 45, No. 2, February 1974
http://hdl.handle.net/10945/44945

Turbulence effects on an ambient pressure discharge

Oscar Biblarz and Robert E. Nelson

Naval Postgraduate School, Monterey, California 93940
(Received 2 July 1973; in final form 19 October 1973)

This work reports on observations of a diffuse discharge in a turbulent air flow. The discharge power was monitored as a function of velocity and turbulence spectrum in a fixed electrode configuration. The flow direction was also reversed to check on the effect of convection. The flow increased the sparking voltage, and turbulence made the current distribution considerably more homogeneous; the discharge power increased from about 1 W with no flow to about 250 W with 60-m/sec grid-generated turbulent flow. This turbulence was most intense in the range between 1 and 10 kHz.

I. INTRODUCTION

Discharges in flowing gases are presently of interest because of their application to electric lasers. Electroaerodynamic or electric discharge convection lasers are important in the high-energy laser field owing to their good efficiency relative to the gas dynamic laser (GDL). Since the gas mixture is essentially dictated by the lasing process, the discharge must be designed with pressure and flow rate as the only variable gas parameters. The cw low-pressure discharge (i.e., in the 1-torr range) with flow rates which allow satisfactory cooling and removal of poisonous byproducts has been successfully operated.[1,2] However, the discharge power is limited by arc breakdown, and this represents an upper limit on the output power of the laser.

The literature in the field of discharges in flowing gases is not particularly extensive. Perhaps the first application of this field was in circuit breakers[3,4] in which convection plays an important part. It is useful to classify flow effects as pure convection and as turbulence even though it is often difficult to separate the two effects. Other work which is primarily convection related is the blowing effect[5] in magnetohydrodynamic channels and corona discharges in electro-gas-dynamic channels.[6]

Turbulence is known to affect discharges[7–9] because, in addition to convection, a great deal of mixing takes place. This mixing is controllable and may offer distinct advantages in the design of discharges. Turbulence has the ability to disperse the discharge, allowing higher currents to exist in a prearcing mode. The turbulent diffusivities can be such that unattractive gases, such as atmospheric air, can be made to accept substantial amounts of electrical power in a diffuse mode discharge. This ability to absorb additional energy is partly due to an increase in the sparking voltage, but the exact mechanisms for the extension of the sparking potential are not fully understood. In this respect, studies of the effects of turbulence on a constricted discharge[10,11] might be helpful.

II. DESCRIPTION OF EXPERIMENTS

The study of grid-generated turbulence on a prearcing atmospheric discharge was made on the facility[12] shown schematically in Fig. 1. In a Plexiglass tunnel three rows of pins, with five pins to a row, and three rows of airfoils were positioned 3.9 cm apart. The pins were located 1 cm away from each other, defining the corners of 1-cm squares. Both the pins and the airfoils were made from aluminum. The screen region was located 1.8 cm upstream of the discharge plane of the 15 pins. The Plexiglass in the test region was slotted to minimize a voltage leakage through a film of moisture that tends to collect at the walls. The Plexiglass allowed convenient viewing of the discharge, and qualitative observations could thereby be made. Atmospheric air, with speeds up to 100 m/sec, was introduced in the test region after passing through one or more screens. It was confirmed with hot-wire measurements that the electrodes were sufficiently removed from the boundary layers so that the important contributors to the turbulence were to be the screens. A spectral analyzer was used to obtain the turbulent energy distributions. The measurements into the analyzer were typically integrated over 4 sec, and a rotation of the hot wire of 90° yielded results substantially unchanged from those prior to rotation. This pointed out a certain degree of one-dimensionality in our measurements. The analyzer outputs 30 discrete frequencies ranging from 25 Hz to 20 kHz. These measurements were made prior to the application of the high voltage.

Various screens were tested. Screen (1), consisting of 20 wires/cm and 0.15-mm-diam wire, produced relative turbulence spectra similar to the no-screen case and therefore was discarded. Screen (2) was made from 0.5-mm-diam brass wire with 7.3 wires/cm; this screen was the most extensively tested. Screen (3) was

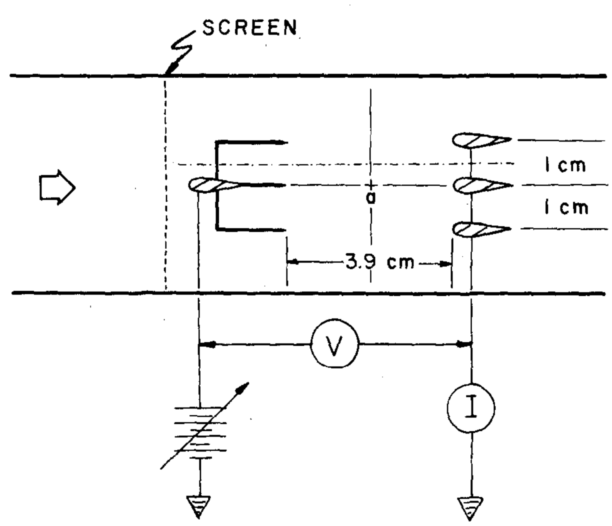

FIG. 1. Schematic of the experimental setup.

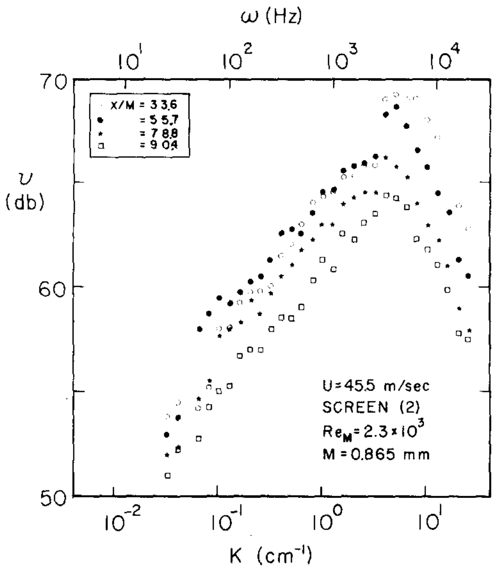

FIG. 2. Spectral decay of turbulence downstream of screen (2).

of the same dimensions as (2) except that it was made out of nylon strands. Screen (4) is not really a screen but a phenolic plate 2.4 mm thick in which 68 holes of 0.6-cm diameter were drilled. This gives the plate a ratio of open area to total area of 50%. The phenolic plate was used only in conjunction with screen (3) and upstream of it. Screens (2) and (3) consisted of square mesh with a grid opening M of 0.865 mm.

In order to understand the nature of the turbulence generated by the screens, various measurements were carried out. The decay of turbulent intensity along the flow direction was measured by using screen (2). The location of these measurements is halfway between the upper and middle airfoil and between pins, as indicated by the dash-dotted line in Fig. 1. The results of the spectral measurement are shown in Fig. 2, where ω is the frequency and K is the wave number obtained by using Taylor's dispersion relation.[10] The peak in the curves is related to the generation and dissipation of turbulent energy. The screens appear to generate turbulent energy above 3000 Hz, and this energy cascades toward higher frequencies (smaller eddies), dissipating more rapidly as the eddy Reynolds number approaches unity. Thus, the region to the left-hand side of the peak decreases primarily in intensity by transfering energy to higher energies, whereas the region to the right-hand side decreases mostly through dissipation. The test region is located relatively close to the mesh, and hence the measurements reflect an initial period of decay (the last station shown in Fig. 2 corresponds to the trailing edge of the airfoils). The decay of the turbulent energy shows a familiar[13,14] trend of decreasing intensity with distance downstream of the mesh, with perhaps some interference from the wakes of the pins. As shown in Fig. 3, all of our data above the peak frequency can be made to collapse into one curve by plotting dimensionless length $x\omega/U$ versus an eddy Reynolds number $v^2/\omega\nu$, where x is the distance from the grid, U is the mean flow velocity, v is the fluctuating velocity, and ν is the kinematic viscosity for air. These spectral data indicate that the rms value of the turbulent velocity decays at a rate which is nearly inversely proportional to x.

The comparison of spectral data between screen (2) and screens (3) and (4) is shown in Fig. 4. The spectra have been normalized so that the peaks match. As will be clear subsequently, the use of screens (3) and (4) together caused an improvement in the discharge over screen (2), and hence the relative distribution of turbulent energies is of interest. In the measurements shown in the figure the hot wire was placed at the midpoint of the interelectrode region (location a in Fig. 1). The combination of screens (3) and (4) shows more intensity at the lower frequencies with as much as 5-dB difference at velocities higher than that represented in Fig. 4. That is to say, the combination of screens (3) and (4) generated the largest most intense eddies. The e^{-1} or -4.3-dB point to the right of the peak gives the scale of the fluctuations, and in Fig. 4 this corresponds to a wave number $K = 17.5\ \text{cm}^{-1}$. Defining l as $2/K$, one

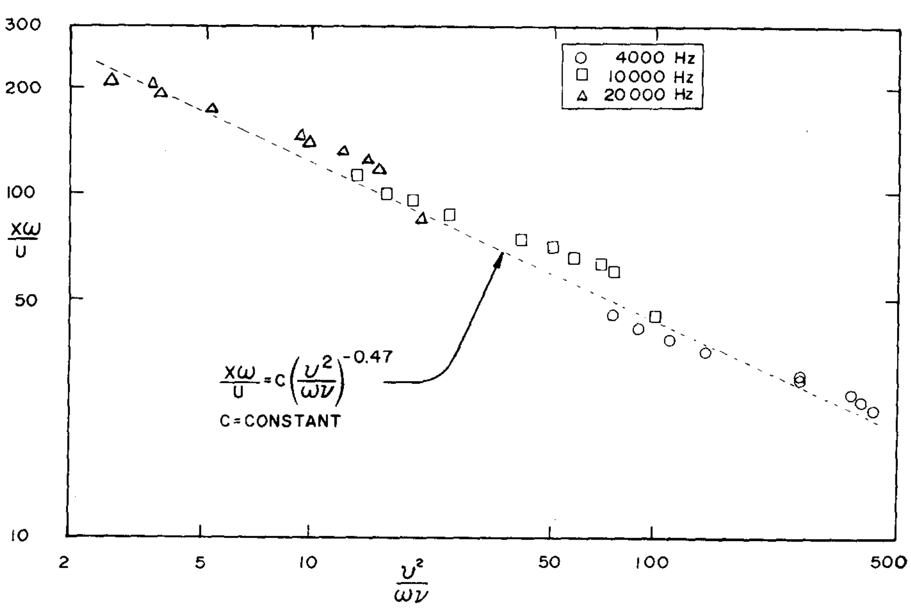

FIG. 3. Spectral turbulence data above 3 kHz.

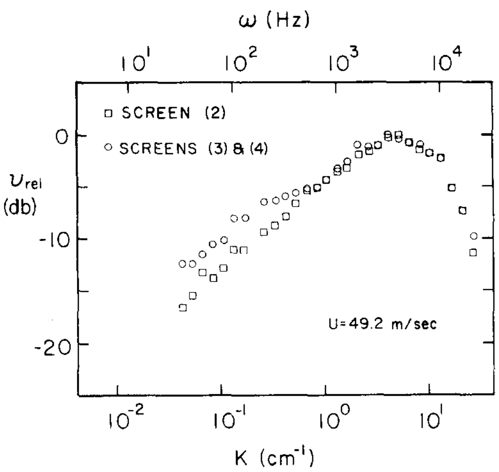

FIG. 4. Comparison of spectral data for screen (2) and screens (3) and (4).

obtains 1.15 mm for the scale of the fluctuations. This scale is of the order of, but slightly greater than, the 0.865-mm grid opening size.

As indicated in Fig. 1, a high-voltage supply initiated a corona discharge between the pins, which were at positive potential, and the grounded airfoils. Positive ions were forced downstream[15] and, because of ion slip in the flow, the results without a screen show that the increase in current due to convection was less than a factor of 2 for the range of speeds tested. A dc power supply was used with a capability of 30 kV and 20 mA. This supply has an output which can be adjusted by changing the impedance before rectification; the ripple of the output voltage is 2%. Current-voltage data were obtained for each run, a run consisting of a particular turbulence spectrum profile derived from a set velocity and mesh configuration. No attempt was made to account for relative humidity changes; it was found, however, that the humidity increased the sparking voltage.[16,17] Since the relative humidity ranged between 10 and 50%, there appeared some scatter in the data obtained with screen (2), the most extensively tested one. The arcing voltage was taken as that voltage at which a filament formed between electrodes (with the subsequent automatic shutoff of the power supply because of the surge of current). The arc usually formed between one of the pins and an airfoil with the pin location being random. The filament was quite bright and it was surmised that the current in the filament consisted of several amps.

III. RESULTS AND DISCUSSION

Figure 5 shows current-voltage data for various runs with turbulence. The no-screen data have very small corona currents and are not included in Fig. 5. Two dashed lines are shown in the figure, one at 23 kV and the other at 26 kV. The former value is representative of the sparking voltage for both the no-flow and the laminar flow cases, whereas the latter is the maximum value of voltage obtained under the test configuration shown in Fig. 1. This 3-kV increase allows a diffuse discharge to exist in a region where the slope of the

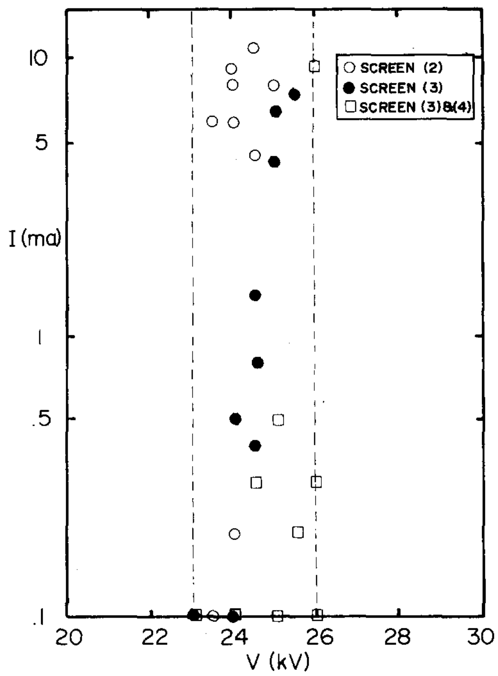

FIG. 5. Current-voltage data with turbulent flow.

current-voltage curve is very steep so that relatively large currents can flow. All the pins appeared to contribute to the current at the higher voltages, and the increase of current was more than 15 times the value without turbulence. Clearly, by delaying the mechanisms of arc formation, there can exist a more energetic corona discharge and this delay can be accomplished by fluid-dynamic means. The primary mechanism involved in the vast current increase seems to be the spreading of the charges due to mixing over the entire interelectrode region. We observed that at the lower levels of turbulence the luminosity of the discharge tended to oscillate; these long-period oscillations could

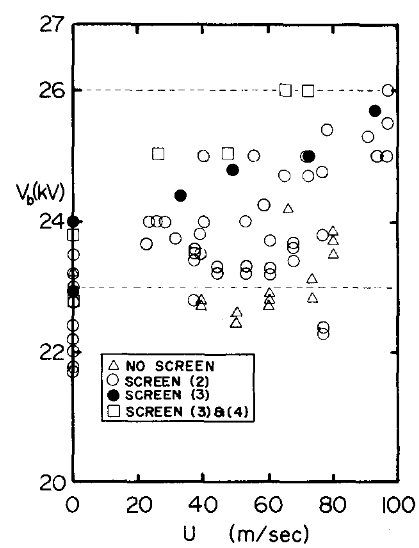

FIG. 6. Sparking voltage vs flow speed.

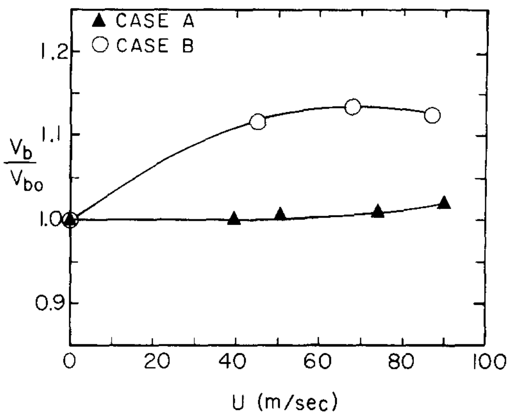

FIG. 7. Convection effect on breakdown voltage as a function of velocity.

also be picked up in the current. With increasing velocity, the higher-intensity turbulence provided for a more stable discharge.

Figure 6 shows the sparking voltage V_b as a function of the mean flow velocity. For a typical set of runs with screen (2), the current near breakdown was 30 μA with no flow, 90 μA with 50 m/sec, 1–5 mA with 72 m/sec, and 10 mA with 92 m/sec. In spite of the data scatter, there is a definite trend of increasing voltage with velocity. The combination of screens (3) and (4) proved that this arrangement could do at 60 m/sec what screen (2) could do at 90 m/sec. Little, if any, difference can be attributed to the fact that screen (2) was metallic. In order to better understand the effect of convection, a separate experiment with the flow direction reversed (case B) was carried out. The airfoil orientation was also reversed to minimize the wakes. The spacing between the electrodes remained at 3.9 cm, and no screens were placed upstream. Results of this case indicate that, whereas the current did not change a great deal from the values obtained with the configuration shown in Fig. 1 (case A), the voltage definitely increased with increasing velocity. The current near breakdown was in the order of 20 μA; the breakdown potential as a function of flow velocity is shown in Fig. 7, where the voltage has been normalized with respect to the no-flow case. The increase in voltage was noticeable throughout the range of velocities tested, in contrast to case A where only a small increase can be seen at 80 m/sec. At this speed, hot-wire measurements indicated that some plenum turbulence was beginning to appear in the test section. It is interesting to note that the increase of breakdown voltage with the screens equaled but did not exceed the maximum value in case B (i.e., a ratio of 1.13).

Our results can be compared with those of Ref. 6 to a limited extent. Reference 6 reports on some experiments with negative charges flowing in a unipolar region with the dimension for electrode separation being 8 mm. They show, in agreement with our work, a more intense breakdown voltage increase when negative charges are flowing with the flow than against the flow for Mach numbers in the range of our experiments (0.1–0.3). The magnitude of the space charge density is not easily surmised for the experimental conditions reported in Ref. 6; moreover, the flow was probably affected by boundary layers and wakes, and no information on the turbulence level is given. Another comparison of our results made with the predictions of Ref. 4 appeared inconclusive. In Ref. 4, calculations of the sparking voltage in a moving gas are given as a function of electron speed and direction with respect to the convecting flow, but neither the trends nor the magnitude predicted are borne out by our experiments.

IV. CONCLUSIONS

It is clear that the turbulent flow has a definite effect on the prearcing discharge. The electron avalanche formation must be affected by the flow via the positive ion motion. The positive ions couple with the flow through collisions with neutrals and, in turn, the electrons couple with the ions via the space charge. The likelihood of negative ion formation and of electron emission from the cathode and the variety of ways that ionization may take place in the gas all make the task of sorting out the effects of turbulence rather difficult. One possibility suggests itself—namely, that the cumulative mechanisms that lead to streamer formation are not isotropic but that they depend on the relative orientation of the electric field to the velocity field. It seems apparent that the net effect of turbulence is more than the extension of the ion paths, and hence it is more than just enlarging the effective length of the interelectrode gap.

The results of our investigation show an increase of power into the diffuse discharge from the no-flow condition (40 μA and 23 kV) to the turbulent condition (9 mA and 26 kV) of about a factor of 250. The combination of screens (3) and (4) appears more efficient in producing the energetic discharge. Observation of the data in Fig. 4 reveals that with this combination of screens more intense turbulence exists at the lower frequencies. Fluctuating velocities as high as 5% of the mean were present during these experiments. If ion motion is being governed by the eddies, then larger eddies can do more complete mixing. No firm conclusions, however, can be made in this regard until we better understand ion slip in turbulence velocity fields[18] and the relations of ion motion to streamer formation.

The effects of different screens and more intense turbulence are yet to be determined. We believe that the improvement reported above can be extended further with some redesign in our apparatus. The possibility of utilizing a turbulent flow to advantage in the design of a laser relaxes the strict requirements presently imposed on the laser gas source. Of course, the effect of this turbulence on laser beam quality will have to be studied once we are able to use turbulence more beneficially in the discharge.

[1]A.C. Eckbreth and F.S. Owen, Rev. Sci. Instrum. 43, 995 (1972).
[2]J.W. Davis and C.O. Brown, AIAA Preprint No. 72-722, 1972 (unpublished).
[3]*Circuit Breaking*, edited by H. Trenchan (Butterworths, London, 1953), Chaps. 2 and 4.
[4]A.E.D. Heylin, Proc. Inst. Electr. Eng. 116, 2101 (1969).
[5]A. Sherman and H. Yeh, Phys. Fluids 11, 96 (1968).
[6]Y.S. Bortnikov, V.A. Nesterov, I.B. Rubashov, and V.I. Chaplii, Sov. Phys.-Tech. Phys. 14, 1579 (1970).
[7]B. Karlowitz, Pure Appl. Chem. 5, 557 (1962).
[8]O. Biblarz, *ENERGY-70 Proceedings* (American Nuclear Society, 1972), Vol. 1, pp. 2–58.
[9]S. T. Demetriades, C.D. Maxwell, G.S. Argyropoulos, and G. Fonda-Bonardi, Eleventh Symposium on Engineering Aspects of MHD, 1970, p. 64 (unpublished).
[10]G.A. Garosi, G. Bekefi, and M. Schulz, Phys. Fluids 13, 2795 (1970).
[11]V.L. Granatstein, A.M. Levine, and M. Subramanian, Phys. Fluids 14, 2581 (1971).
[12]R.E. Nelson, M.S. thesis (Naval Postgraduate School, 1973) (unpublished).
[13]J.D. Hinze, *Turbulence* (McGraw-Hill, New York, 1959), Chap. 3.
[14]H.L. Dryden, G.B. Schubauer, W.C. Mock, Jr., and H.K. Skramstad, NACA Report No. 581, 1937 (unpublished).
[15]Reversing the polarity of the electrodes increases the breakdown voltage, but we chose not to pursue this electrical configuration in our experiments.
[16]J.D. Cobine, *Gaseous Conductors* (Dover, New York, 1958).
[17]L.B. Loeb, *Basic Processes of Gaseous Electonics* (University of California Press, Berkeley, 1960).
[18]O. Biblarz, *7th Intersociety Energy Conversion Engineering Conference*, 1972 (American Chemical Society, Washington, D.C., 1972), p. 1169.